Vortex dynamics differences due to twin-boundary pinning anisotropy in $YBa_2Cu_3O_x$ at low temperatures for $H \| ab$ planes

S. Salem-Sugui, Jr.,[1] A. D. Alvarenga,[2] M. Friesen,[3] K. C. Goretta,[4] O. F. Schilling,[5] F. G. Gandra,[6] B. W. Veal,[7] and P. Paulikas[7]

[1]*Instituto de Física, Universidade Federal do Rio de Janeiro C.P.68528, 21945-970 Rio de Janeiro, RJ, Brasil*
[2]*Centro Brasileiro de Pesquisas Fisicas, Rua Dr. Xavier Sigaud, 150, 22290-180 Rio de Janeiro, RJ, Brazil*
[3]*Department of Materials Science and Engineering, 1500 Engineering Drive, University of Wisconsin, Madison, Wisconsin 53706, USA*
[4]*Energy Technology Laboratory, Argonne National laboratory, Argonne, Illinois 60439-4838, USA*
[5]*Departamento de Física, Universidade Federal de Santa Catarina, 88040-900 Florianopolis, SC, Brazil*
[6]*Instituto de Fisica, UNICAMP, CP6185, 13083-970 Campinas, SP, Brazil*
[7]*Materials Sciences Division, Argonne National Laboratory, Argonne, Illinois 60439-4838, USA*

(Received 22 August 2003; revised manuscript received 1 September 2004; published 6 January 2005)

We measured the magnetization M of a twin-aligned single crystal of $YBa_2Cu_3O_x$ (YBaCuO), with $T_c = 91$ K, as a function of temperature T and magnetic field H, with H applied along the ab planes. Isothermal M-vs-H and M-vs-time curves were obtained with H applied parallel ($\|$) and perpendicular ($\perp$) to the twin boundary (TB) direction. M-vs-H curves exhibited two minima below 38 K, which resembled similar curves that have been obtained in YBaCuO for $H \| c$ axis. Above 12 K, the field positions of the minima for $H \|$ TB and $H \perp$ TB were quite similar. Below 12 K, the position of the second minimum $H_{\min}$ occurred at a higher field value with $H \|$ TB. Below 6 K, only one minimum appeared for both field directions. At low temperatures, these minima in the M-vs-H curves produced maxima in the critical current. It was determined that vortex lines were expelled more easily for $H \|$ TB than for $H \perp$ TB and, therefore, below a certain field value, that $J_c(H \perp \text{TB})$ was larger than $J_c(H \| \text{TB})$. At $T < 12$ K with $H \|$ TB, the relaxation rate for flux lines leaving the crystal was found to be different from that for flux entering the crystal. We also observed flux jumps at low temperatures, with their sizes depending on the orientation of magnetic field with respect to the TB's.

DOI: 10.1103/PhysRevB.71.024503 PACS number(s): 74.72.Bk, 74.25.Qt, 74.25.Ha, 74.62.Dh

I. INTRODUCTION

Twin planes are ubiquitous in the high-temperature superconductor $YBa_2Cu_3O_x$ (YBaCuO). Under microscopic analysis they appear as flat, slablike domains of micrometer thickness. The domains are coherent and are oriented in various [110] directions. The a and b axes are inverted in neighboring domains. The domain boundaries are commonly referred to as twin boundaries (TB's). The boundary region has a structure different from that of the bulk crystal, including a relative deficiency of oxygen[1–3] or excess of impurities that can accumulate during crystal growth. TB's form strong vortex pinning centers and are responsible for a rich variety of transport anisotropies. Under typical growth conditions, these anisotropies cannot be observed readily because the neighboring TB's are not aligned. The gross vortex dynamics of samples with such TB's are determined by the sample's texture. Twin-aligned YBaCuO samples can, however, be formed, and such samples provide windows into the effects on superconducting properties of TB's.

Initial studies of twin-aligned YBaCuO single crystals revealed strong anisotropies for magnetic fields perpendicular to the c axis of the crystal, $H \perp c$, for TB's oriented either parallel or perpendicular to the field.[3–6] These studies included isothermal measurements of resistivity and magnetic hysteresis. Additional angular dependences between H and TB's were reported in Refs. 7 and 8. The effects of TB's on vortex dynamics were studied by magneto-optical measurements for H parallel and perpendicular to the c axis.[9–11] More recent studies of twin-aligned single crystals of YBaCuO include transport measurements as a function of current in the ab plane[12] and Bitter decoration experiments under tilted magnetic fields.[13] Vortex-pinning[14] and flux-creep measurements have been studied through use of ac probes for the configurations H parallel to the TB's, $H \|$ TB, and H perpendicular to the TB's, $H \perp$ TB.[15]

Previous TB-based studies of YBaCuO focused mainly on higher temperatures, which motivated the present work in the temperature region $50\ \text{K} < T < 2$ K. We studied the effects of TB pinning anisotropy on magnetic-hysteresis and magnetic-relaxation curves for a twin-aligned single crystal of YBaCuO, with the magnetic field applied in the ab plane for two directions: namely, $H \|$ TB and $H \perp$ TB. The study revealed interesting features in magnetic hysteresis and magnetic relaxation curves due to TB vortex-pinning anisotropy, which, to our knowledge, have not yet been reported: We observe the existence of a second minimum in magnetic hysteresis curves below 38 K, which temperature behavior below 12 K for $H \|$ TB is quite different than the one observed when $H \perp$ TB. The temperature behavior (below 12 K) of the relaxation rate for $H \|$ TB (studied for $H = 3$ T) is also quite distinct from the behavior observed when $H \perp$ TB. At low temperatures, maxima in the critical current J_c occurred at the positions of the minimums in the $M(H)$ curves. We also observe flux jumps in the magnetization curves at low temperatures, with sizes depending whether H is applied parallel or perpendicular to TB's.

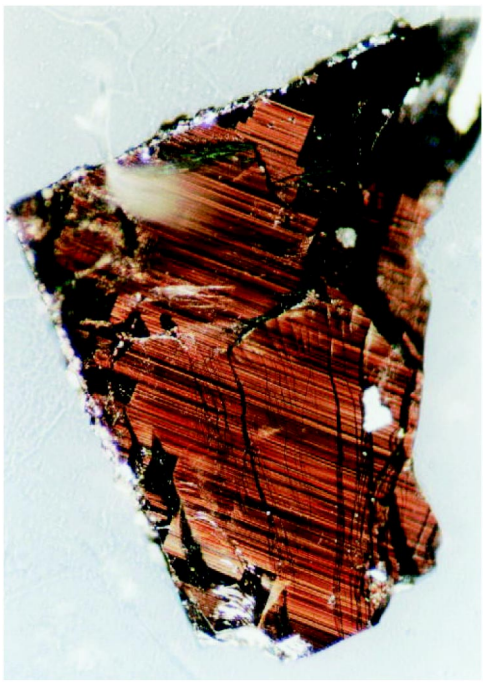

FIG. 1. Microscopic photo of the sample (100× enlarged), evidencing paralell twin boundaries along the surface. The photo was obtained by adjusting the incident angle of the light into the sample's surface to the Brewster angle, allowing the observation of the twin-plane orientation.

Flux jumps result from thermomagnetic instabilities associated with dissipative heating (either flux flow or avalanche). If the dissipative heating cannot diffuse through the sample, it can increase the local temperature, possibly even above the critical temperature T_c, producing a jump in magnetization. Such jumps may occur in response to changes in the external field if the magnetic-diffusion time is shorter than the thermal-diffusion time. The size of a jump depends on the rate of magnetic field increase, dH/dt. Theoretically, the stability criterion[16,17] defines a critical thickness below which flux jumps do not occur. Experimentally, such results have been confirmed for melt-textured YBaCuO with the magnetic field applied perpendicular to the c axis, $H \perp c$.[18] Additional asymmetries have been observed in the different branches of magnetization hysteresis curves, $M(H)$, for melt-textured YBaCuO at $T < 6$ K, with a greater prevalence of flux jumps occurring with increasing field than with decreasing field.[18] These results are in contrast to those for $H \| c$, for which no hysteresis asymmetries have been observed.[18,19] For practical applications, especially those involving high currents, characterization and management of flux jumps become critical. We therefore analyzed the observed flux jumps in some detail.

II. EXPERIMENTAL DETAILS

The sample was a single crystal of YBaCuO with $T_c = 91$ K and dimensions $\sim 1 \times 1 \times 0.1$ mm. Figure 1 shows an enlarged (100×) photo of the sample's surface. All twin boundaries within the crystal were parallel and extended across the entire thickness of the sample, as confirmed by microscopic analysis. The density of TB's was estimated to be 45 twins per mm. The sample had an approximately square shape, with one slightly rounded corner, and the twin boundaries displaced perpendicular to the larger diagonal.

Magnetization and magnetic-relaxation data were taken after cooling the sample in zero applied magnetic field. A commercial magnetometer (Quantum Design PPMS-9T) was utilized for the measurements. The magnetic signal of the sample (plus sample holder) was obtained from the inductive signal of a pickup coil, which appeared because of motion of the sample through the coil in a homogeneous magnetic field, which we term a scan. Each set of magnetization data represents the average of three scans. Magnetization-vs-field $M(H)$ curves were obtained at fixed temperatures ranging from 2 to 50 K. For a fixed applied field of $H = 3$ T, magnetic-relaxation measurements were obtained at 60-s intervals over a period of 3600 s, for both the upper and lower branches of a hysteresis curve. The remanent magnetization at zero field was also recorded. The value of 3 T was chosen to minimize the effects of field penetration during the measurements.[20] We refer to the increasing field magnetization as M_{in}, the decreasing field magnetization as M_{out}, and the remanent magnetization as M_{rem}. The latter two signals were obtained after first increasing the field to 9 T.

In the temperature range 2–12 K, all relaxation measurements were obtained for both field orientations with respect to the TB's. Care was taken to assure that the magnetic field was applied in the *ab* plane. The sample was mounted on a flat surface machined into the center of a 3-cm wooden cylinder that fit snugly into a straw that was inserted into the magnetometer. An optical microscope with polarized light was used for sample mounting. The angle between the TB's and the magnetic field H was estimated to be accurate to $< 2°$. After the experiment was concluded, we measured $M(H)$ for the sample holder at all relevant experimental temperatures to account for background corrections.

III. RESULTS AND DISCUSSION

Figure 2 contains selected M-vs-H curves obtained for both orientations of H with respect to the TB's at $T = 25$, 15, and 8 K. The arrows in Fig. 2 are pointed at the curves obtained at 8 K. From left to right in the figure, they are the following: the first arrow is the first minimum H_{pen}, which is associated with field penetration; the second arrow is the local maximum H_{on}, which is associated with the field at which pinning sets in; and the third and fourth arrows are the second minima H_{min}, which are reminiscent of the second magnetization peaks observed in high-T_c superconductors for $H \| c$ axis. The decreasing-field portions of M-vs-H curves do not show any maximum. The third and fourth arrows show, respectively, H_{min} for $H \perp$ TB and H_{min} for $H \|$ TB. These three fields—H_{pen}, H_{on}, and H_{min}—were clearly present in all M-vs-H curves obtained at 8–33 K.

M-vs-H curves obtained at or above 38 K exhibited only a single minimum, which is associated with H_{pen}. M-vs-H curves obtained below 8 K also exhibited only one minimum, which, in this particular case, may possibly be associ-

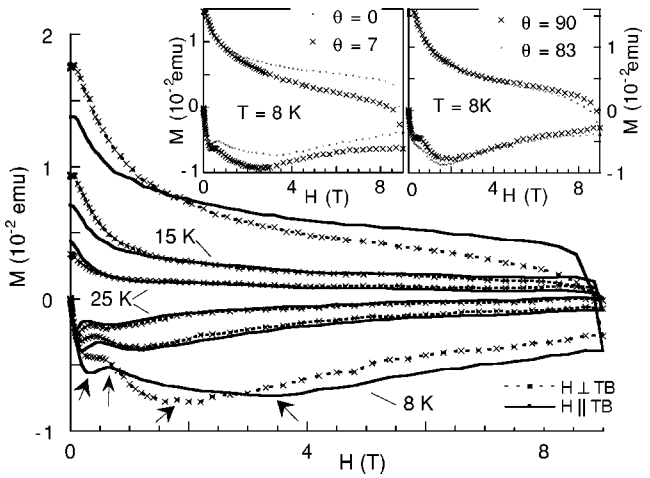

FIG. 2. Selected M-vs-H curves at 25, 15, and 8 K for $H\|$TB and $H\perp$TB; insets show curves at 8 K after changing the angle between H and the TB's by $\sim 7°$.

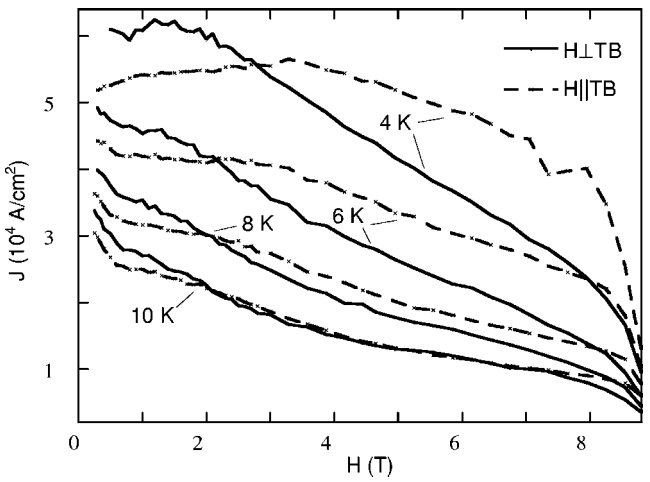

FIG. 4. J_c vs H curves, as estimated from $M(H)$ curves obtained below 10 K for $H\|$TB and $H\perp$TB.

ated with $H_{\min}$. This conjecture will be discussed below.

The positions of H_{pen}, H_{on}, and $H_{\min}$ for both directions of applied field were approximately the same for temperatures $12\ \text{K} < T < 38\ \text{K}$, but a change in the field position of $M_{\min}$ was noted below 12 K. Such a change in field position can be observed in the $M(H)$ curves at 8 K depicted in Fig. 2, in which $H_{\min}$ for $H\|$TB occurred at a much higher field than did $H_{\min}$ for $H\perp$TB. The physical reason for the shifting of $H_{\min}$, as shown at 8 K, to occur only below 12 K is not clear. It may be related to the temperature behavior of the TB barriers found below 12 K, as will be discussed below. The insets in Fig. 2 show the angular dependence at 8 K of $M(H)$ for small angles. These data will also be discussed below.

Figure 3 shows $M(H)$ curves obtained at 2 K in the main figure and at 4 K in the inset. These curves clearly show the existence of a single minimum. As observed for $H_{\min}$ at 8 K, the field position of the minimum is higher for $H\|$TB than for $H\perp$TB, which suggests that the minimum observed below 8 K is associated with $H_{\min}$ rather than with H_{pen}. The

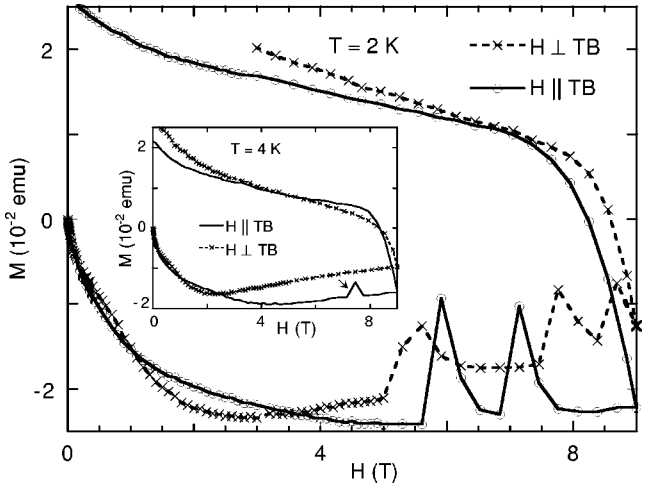

FIG. 3. M-vs-H curves for $H\|$TB and $H\perp$TB at 2 K (inset at 4 K).

inflection points apparent in the curves of Fig. 3 for fields $H < H_{\min}$, which are most visible in the $H\perp$TB curves, are possibly related to H_{on}. Flux jumps are also evident for $H\|$TB. A smaller flux jump was also observed at 4 K (inset of Fig. 3) for $H\|$TB only.

The principal differences that are due to TB's among the curves in Fig. 2 and between those in Fig. 3 at fixed temperatures are as follows.

(1) The values of ΔM for intermediate and higher fields were higher for $H\|$TB than for $H\perp$TB. This result been obtained before; it is due to twin-boundary pinning.[3]

(2) The diamagnetic signal for $H < H_{\text{pen}}$ was higher for $H\|$TB than for $H\perp$TB. This result has been also observed previously.[3] For the same applied field value H, differences in the diamagnetic signal in the field-penetration region, just above H_{c1}, suggest that the local field H_i at the sample surface is smaller when $H\perp$TB than when $H\|$TB. Such a result is possible if the demagnetization factor of the sample is higher for the configuration $H\perp$TB: $H_i = H - NM$, where N is the demagnetization factor. Our sample was a thin slab and the experiment was conducted with the magnetic field lying in the plane of the slab. This configuration suggests that demagnetization fields were quite small. On the other hand, although the crystal's face was approximately square, one corner was rounded, with the twin boundaries displaced perpendicular to the larger diagonal. Therefore, the sample geometry for $H\|$TB was significantly different than for $H\perp$TB, and the demagnetization factor for each case would be expected to be different, which may explain the differences in the diamagnetic signal observed for each case.

(3) After decreasing the field until $H=0$ (the decreasing-field branches of the M-vs-H curves), the remanent magnetization defined as $M(H=0)$ was higher for $H\perp$TB than for $H\|$TB.[3] In fact, magnetization in the decreasing-field branch started to become higher for $H\perp$TB below a certain field, the value of which increased as temperature decreased. This response was observed for all $M(H)$ curves and can be clearly observed in Fig. 4, in which the estimated critical current density J_c vs field is plotted for temperatures below 10 K, for both field directions with respect to the TB's. J_c in

A/cm^2 was estimated from the Bean critical-state model.[21] Below a certain field, J_c for $H \perp$ TB was always higher than J_c for $H \parallel$ TB; this response was observed for all curves from 50 K to 2 K. This relationship between J_c and the TB's does not appear to have been discussed in the literature. It is interesting to note that as temperature was lowered, at a field of a few tesla a broad maximum in J_c emerged (maxima were clear at 4 K). The position of each maximum in J_c appeared to be related to the respective field position of the minimum (H_{min}) in each $M(H)$ curve at 4 K.

After obtaining the data set at 2–50 K, we measured $M(H)$ curves at 8 K, with the applied magnetic field tilted within the plane by a small angle ($5° < \theta < 10°$) relative to the original directions, $H \perp$ TB ($\theta = 90°$) and $H \parallel$ TB ($\theta = 0°$) (The magnetic field remained in the *ab* plane when the sample was rotated.) Although a full set of angular-dependence measurements was beyond the scope of this work, this limited set of measurements allowed us to check for possible edge (or geometric) effects in the $M(H)$ curves at temperatures at which two minima had been clearly resolved. The results for each set of $M(H)$ curves are shown in the insets of Fig. 2. Inspection of the insets reveals two facts.

(a) Rotation of the TB's by a small angle with respect to the applied field changed the position of the second minimum for $H \parallel$ TB (H_{min} was displaced by a small field value after the sample was rotated), but not for $H \perp$ TB. Change of the position of H_{min} only for the case $H \parallel$ TB suggests that H_{min} is related to TB pinning anisotropy. We further speculate that the absence of the corresponding second peak in the decreasing-field branch of the curve may be due to the fact that with decreasing of the field, flux lines could leave the sample relatively easily through the TB's.

(b) Rotation of TB's with respect to the applied field by a small angle had considerable effect on the shape of the $M(H)$ curves in the field-penetration region ($H_{pen} < H < H_{on}$) for both $H \perp$ TB and $H \parallel$ TB, which provides evidence for the importance of edge (or geometric) effects in this field region. The $M(H)$ curve for $\theta = 7°$ (left inset of Fig. 2) is apparently rotated with respect to the $M(H)$ curve for $\theta = 0°$ in the same figure. This apparent rotation in the $M(H)$ curve is simply due to a change in the position of the sample in the holder: After rotating the sample, it was displaced out of the middle of the its holder, and the signal due to the sample holder (i.e., the background magnetization) was not subtracted correctly, which produced the apparent rotation. In our experimental setup, the sample was fixed to the sample holder with GE varnish. Changing the sample's position necessitated diluting the varnish, rotating the sample, and then reattaching the sample at the exact correct position. A full angular-dependence experiment would require the sample to be fixed to an appropriate rotator, to avoid the possibility of sample damage.

Differences between the curves with $H \parallel$ TB and $H \perp$ TB of Figs. 2 and 3, as listed above in itens (1) and (3), can be explained by the following considerations. (1) There is a vortex line along the magnetic field direction; i.e., there are no pancake vortices in the *ab* planes. (2) Defects located at the boundaries of the twin planes act as pinning centers and also prevent vortices from crossing the TB's when $H \parallel$ TB. (3) For intermediate and higher fields, the density of vortex lines pinned with increasing and decreasing applied field is higher for $H \parallel$ TB than for $H \perp$ TB. This final contention can be obtained after comparison of the values of magnetization in the increasing (decreasing) field of a curve obtained for $H \parallel$ TB with the corresponding (at same temperature) curve obtained for $H \perp$ TB, as well by comparing the respectives values of $\Delta M(H)$ of both curves. As a consequence of the preceding facts, the average distance between vortex lines, for intermediate and higher fields, is smaller for $H \parallel$ TB than for $H \perp$ TB.

The vortex-vortex interaction energy[22] is given by $F_{12} = (\phi_0^2 / 8\pi^2\lambda^2) K_0(r_{12}/\lambda)$, where ϕ_0 is the quantum flux, λ is the penetration depth, r_{12} is the average distance between vortex lines, and K_0 is a zeroth-order Hankel function of imaginary argument. The interaction given by F_{12} is repulsive, and the repulsive force between vortex lines (given by $-\partial F_{12}/\partial x$ for the x direction) increases as r_{12} decreases. An imbalance between $-\partial F_{12}/\partial x$ and the magnetic pressure may produce vortex motion which, in the case of decreasing of the field, produces vortex exit. From the above considerations, the repulsive force is higher for $H \parallel$ TB than for $H \perp$ TB.

By assuming a triangular lattice of vortex lines (it is also assumed that only the boundary regions of the TB plane can strongly pin a vortex), the repulsion between vortex lines after decreasing the applied magnetic field may produce vortex motion in two directions approximately perpendicular to each other and both perpendicular to the applied magnetic field. When $H \parallel$ TB, one direction of repulsion produces a motion that drives the vortices to cross the TB's, and the other direction produces a motion that drives the vortices to move between the TB plane. Then, when $H \parallel$ TB and the field is decreasing, the TB barriers prevent the vortices crossing the TB's, and the vortex motion occurs preferentially between the TB's (in this sense, one might consider that the TB planes act as channels for exit of vortices). When $H \perp$ TB, the directions of the repulsion between vortex lines are both paralell to the TB planes, but in this case, a vortex line is strongly pinned by TB's oriented perpendicular to the vortex line. Furthermore, when field is decreasing, one may expect that it is easier for vortices to leave the sample for $H \parallel$ TB than for $H \perp$ TB, as was observed in relaxation data for $H = 3$ T. Since vortices can exit the sample easily when $H \parallel$ TB, one may expect that below a certain applied field, the magnetization in the decreasing-field branch for $H \parallel$ TB may eventually become smaller than the magnetization in the decreasing-field branch for $H \perp$ TB at same temperature, as observed in M-vs-H curves of Figs. 2 and 3.

The values of H_{min}, H_{on}, and H_{pen}, as obtained from the $M(H)$ curves, are plotted in Fig. 5. The curves drawn for H_{min} and H_{on} are only to guide the eye. Below 12 K, the values of H_{min} increased dramatically for $H \parallel$ TB and became substantially larger than those for $H \perp$ TB. Above 12 K, the values of H_{min} were approximately the same for both directions of applied magnetic field. The values of H_{on} were also approximately the same for both field directions. Below 12 K, the values for $H \parallel$ TB became measurably larger than those for $H \perp$ TB. This trend was the same as observed for H_{min}, but the relative differences were much less.

There was little difference between the values of H_{pen} for the two field directions. It was found that the values of H_{pen}

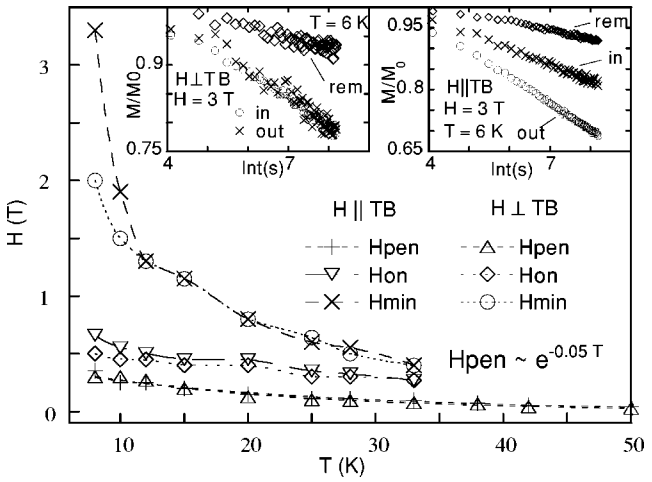

FIG. 5. H_{pen}, H_{on}, and H_{min} vs T; insets show magnetic-relaxation curves at 6 K and $H=3$ T (in and out) and for $H=0$ (rem) for $H\|$TB and $H\perp$TB.

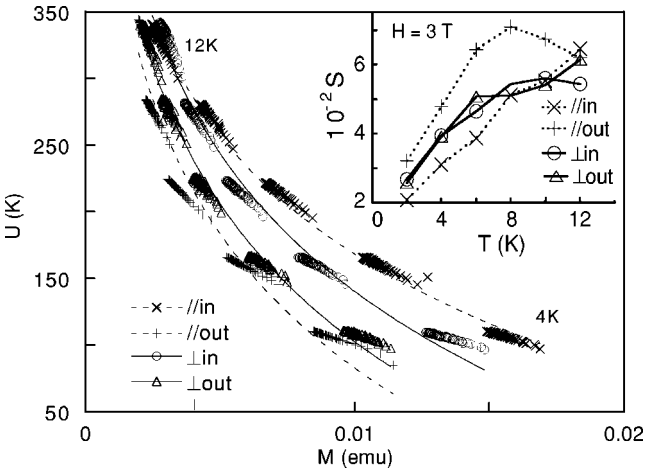

FIG. 6. Effective activation energy U for flux in and flux out for $H=3$ T vs $|M|$ for $H\|$TB and $H\perp$TB. Solid and dotted lines represent fits of $U\sim\ln|M|$ and the inset shows rate of relaxation S vs T for the relaxation-data set obtained for $H=3$ T.

for both field directions could be fitted well by an exponential expression. An exponential response of H_{pen} with temperature has been observed by de Andrade *et al.* for anisotropic layered superconductors when H was applied along the c-axis direction, perpendicular to the ab layers.[23] In that study, the exponential behavior was interpreted in terms of surface barriers appearing because of the existence of pancakelike vortices lying between the layers. In the present study, the field was applied along the ab planes and there were no pancakelike vortices lying between the layers.

The effects of TB's on vortex phenomena can be investigated most directly through dynamics studies. We performed flux-creep studies, emphasizing the anisotropy of flux dynamics with respect to the TB's. Measurements concentrated on temperatures below 12 K, because the main effects of the TB's were observed in this temperature regime. The insets of Fig. 5 show magnetic-relaxation curves $M(t)$ obtained at 6 K with $H=3$ T for both directions of the applied magnetic field. The curves were obtained for the increasing- and decreasing-field branches and for $H=0$ after the field was discharged (M_{rem}). All $M(t)$ curves presented an approximately linear response versus the logarithm of time. It is interesting to note the large noise in $M_{rem}(t)$ and also (although not as large) in $M_{out}(t)$ for $H\perp$TB. In comparison, $M_{rem}(t)$ and $M_{out}(t)$ were quite consistent for $H\|$TB. Such differences in noise were observed at all temperatures. The noise in the relaxation measurements seems to be related to the resolution of the measurement, and the fact that a vortex can exit much more easily when $H\|$TB (large magnetic relaxation) produced less noise in this case. The insets of Fig. 5 also reveal large differences between $M_{in}(t)$ and $M_{out}(t)$ for $H\|$TB (but not for $H\perp$TB). The insets of Fig. 5 also reveal a large difference in $M_{in}(t)$ and $M_{out}(t)$ values between $H\|$TB and $H\perp$TB.

We estimated the current densities J at 6 K generated during the initial stage of magnetic relaxation $M(t=0)$ until $M(t=60-120$ s) for the curves shown in the insets of Fig. 5. For a fixed field H applied along the z direction, in Gaussian units, $\partial B_z/\partial x=-4\pi J/c\sim 4\pi\partial(M-M_{eq})/\partial x\sim 4\pi(dM/dt)\times(dt/dx)$, where M_{eq} is the equilibrium magnetization and dx/dt is the flux velocity (which is on the order of cm/s).[22] Because we did not make local magnetization measurements (our data were obtained over the entire volume of the sample), we consider that $dM_{eq}/dx\sim 0$. From the experimental values of dM/dt (in emu/cm^3 s) and by assuming $dx/dt=1$ cm/s, the estimated values of J were (1) $H\|$TB: 0.41 A/cm^2 (flux in), 0.51 A/cm^2 (flux out), and 0.17 A/cm^2 (remanent); (2) $H\perp$TB: 0.32 A/cm^2 (flux in), 0.32 A/cm^2 (flux out), and 0.13 A/cm^2 (remanent).

A current value of 0.51 A/cm^2 (the largest current density that was estimated above) corresponds to a transport current of 5 mA across the largest area of the crystal (1×1 mm^2 face), and to 0.5 mA across the smallest area (1×0.1 mm^2 face). We note that after 30 min of relaxation, dM/dt decayed to values 30–50 times smaller than those initially calculated. The flux velocity would also be expected to decay accordingly.[24]

Before analyzing the rate of the magnetic relaxation, it is important to obtain the effective activation energy $U(M)$. According to Maley *et al.*,[25] $U(M)$ be obtained from $U(M)/k_B=-T\ln|d(M-M_{eq})/dt|+T\ln(B\nu a/\pi d)$, where ν is the attempt frequency, a is the flux hopping distance, and d is the sample thickness. The equilibrium magnetization M_{eq} is estimated as the average $(M^+ + M^-)/2$, where M^+ and M^- are, respectively, the magnetization in the increasing- and decreasing-field branches of the hysteresis curve.[25] Values of M_{eq} were found to be less than 10% of M, and we therefore plotted $U(M)$ vs $|M|$ instead $|M-M_{eq}|$, for $M_{in}(t)$ and $M_{out}(t)$ and for both directions of applied magnetic field (Fig. 6). Each set of data in Fig. 6 reflects a $M(t)$ curve and each point $(U(M),M)$ in a set was obtained by first calculating $T\ln|dM/dt|$. The final value of $U(M)$ is obtained by adjusting a value of the constant $C=\ln(B\nu a/\pi d)$ that produced a smooth fit (dotted and solid lines in Fig. 6) to the data obtained for a given configuration and fixed magnetic field. For all curves of Fig. 6, $C=12$. This same value of $C=12$ was reported previously for a YBaCuO single crystal.[26]

For $C=12$, $d=0.1$ mm (the thickness of the crystal), and $B\sim 3T$, $\nu a\sim 4.7$ cm s^{-1}, which is consistent with a flux hop-

ping distance $a=10$ nm and an attempt frequency $\nu=4.7\times10^6$ Hz. Each line in Fig. 6 represents a fit of $U\sim\ln|M|$. With the exception of $U(M_{\text{out}})$ for $H\|$TB, data from 4 to 12 K for the other three configurations fall very close to the respective $\ln|M|$ line. Logarithmic decreasing of U with increasing M is consistent with the linear dependence of M with the logarithm of *time*, as was observed. Data at $T=2$ K, the lowest temperature of measurement, did not follow the smooth logarithmic fit and are not shown. Figure 6 reveals that the responses of $U(M_{\text{in}})$ and $U(M_{\text{out}})$ were quite similar for $H\perp$TB (in the sense that data follow the $\ln|M|$ behavior) but not for $H\|$TB for which only $U(M_{\text{in}})$ follow the logarithimic behavior with M. The differences for $H\|$TB explain the differences in $M_{\text{in}}(t)$ and $M_{\text{out}}(t)$ (and also in the rate of relaxation discussed below) observed for $H\|$TB, as shown in the inset of Fig. 5.

One may obtain graphically the so-called apparent pinning energy U_0 by constructing a tangent to a given data set in a given $U(M)$ curve (such as in Fig. 6), where U_0 is the value at which the tangent intercepts the y axis. This value can also be obtained by the expression $U_0=-k_BT/S$, in which $S=(1/M_0)(d|M|/d\ln t)$ and S is the relaxation rate and M is the magnetization at time $t=0$.[27] The U_0 value obtained by such a graphical means is 50% higher than $U_0=-k_BT/S$, which may likely indicate that U_0 is not well defined for the crystal used in this study.

Because of this consideration, instead of U_0, we examined the relaxation rates S for M_{in} (S_{in}) and M_{out} (S_{out}). The inset of Fig. 6 contains plots of S_{in} and S_{out} for both directions of applied magnetic field. In this inset, the symbols $\|$in and $\|$out denote S_{in} and S_{out} for $H\|$TB, and $\perp$in and $\perp$out denote S_{in} and S_{out} for $H\perp$TB. As in Fig. 6 proper, the curves for S_{in} and S_{out} for $H\perp$TB were similar, which provides further evidence of the flux dynamics being approximately independent of the hysteresis branch (increasing or decreasing) in this test configuration. On the other hand the responses versus temperature of S_{in} and S_{out} for $H\|$TB confirmed that the barrier for vortices leaving the sample was lower for this configuration. Comparison between S_{out} values for both configurations also indicated that the barrier for vortices leaving the sample was lower for $H\|$TB than for $H\perp$TB.

The relaxation rates with increasing field in the $H\|$TB configuration were smaller than in the $H\perp$TB configuration. This difference might be related to the changes in the position of H_{min} observed for $H\|$TB below 12 K.

The differences between various sets of curves disappeared as T approached 12 K; above 12 K, the $M(H)$ curves were quite similar for both TB configurations. These results suggest that the TB's had a weaker effect on flux dynamics above 12 K. It is interesting to note that surface barriers are expected to produce a similar asymmetric, but inverted, responses for S_{in} and S_{out} as shown in the inset of Fig. 6 for the configuration $H\|$TB.[28]

We finally discuss the flux jumps observed at low temperatures. The data at 2 K (Fig. 3) show the larger magnitude of the flux jumps when $H\|$TB, and the data at 4 K (inset of Fig. 3), for which a flux jump only occurred in the hysteresis curve for $H\|$TB, show the same trend. No flux jumps occurred above 4 K (Fig. 2 and other data not presented in the figures).

It is likely that flux jumps appear due to a continuous imposed dH/dt. On the other hand, data were collected at a fixed value of H which was reached for a fixed value of $dH/dt=0.02$ T/s. In the field region in which flux jumps were observed, magnetization was measured in intervals of 0.3 T. Upon analyzing the time between two consecutive data points, with $\Delta H=0.3$ T, we concluded that the value of 0.02 T/s was not achieved in an interval of 0.03 T. The built-in program used to charge the magnet probably increased dH/dt to a maximum value, which depended on ΔH, and then rapidly decreased dH/dt as ΔH approached its limit. (In the analysis, we assumed that the ramping of dH/dt was reproducible for a given ΔH.)

Magnetization was measured at a fixed field—i.e., $dH/dt=0$—and therefore a given flux jump might appear smaller than it would if the value of ΔH were larger. For this reason, we did not repeat the measurements with larger values of ΔH.

Obtaining data with various values of dH/dt is desirable once flux jumps (size, number, and value of the first applied field at which one occurs) are dependent on dH/dt. From Fig. 3 one may observe that after a flux jump occurred, a few increments of ΔH were required for the curve to return to an extrapolation of its previous path. This fact suggests that the actual size of each flux jump (as would be obtained from an experiment with a continuously varying field dH/dt) was close to the size that was observed in our experiments.

The data in Fig. 3 strongly suggest that there was flux-jump anisotropy with respect to the TB's. To our knowledge there has been no previous report of flux jumps in twin-aligned single crystals of YBaCuO. Systematic studies of the first flux jump and its reproducibility and size, obtained with satisfactory statistics, are planned. This work requires continuous varying of dH/dt.

We estimated the heat generated by the first flux jump at 2 K (Fig. 3). The dissipation that heats the sample can be calculated by $\int_0^{H_1} M dH=\int_2^{T_f} C_v dT$. The first expression is strictly applicable for a total flux jump that heats a sample to the normal state, which was not the case in our measurements. The second expression, the integral of $C_v dT$ from the initial temperature to the final temperature T_f, can be evaluated by using published values of the specific heat of YBaCuO ($T_c=90$ K) as a function of temperature for fixed fields.[29] By plotting $M(H)$ curves for a given field orientation at 2, 4, 6, and 8 K, we obtained an approximate value for the temperature reached by the first flux jump that occurred at 2 K. The first flux jump for $H\|$TB occurred at $H\sim6$ T. It heated the sample to ~6 K; the estimated energy of the heating was 2.8×10^{-8} J. The first flux jump for $H\perp$TB occurred at $H\sim5$ T. It heated the sample to ~4 K; the estimated energy of the heating was 7.3×10^{-9} J. The heating produced with $H\|$TB was almost 4 times larger than that produced when $H\perp$TB.

Based on the these vortex-dynamics data, differences in the sizes of flux jumps depending on whether $H\|$TB or $H\perp$TB are to be expected. Because the TB's constitute an especially strong pinning center in the configuration $H\|$TB, a vortex can be pinned along its entire length. Under increasing magnetic pressure, the vortices eventually pour in, similar to an avalanche, which may induce a heating instability.

In contrast, with $H \perp$ TB, the vortices pass through a given TB at one point only, forming a weaker pinning center and inducing a smaller effect on the vortex dynamics. Indeed, from Fig. 3 it is clear that flux jumps in the $H \perp$ TB configuration were smaller than in the $H \parallel$ TB configuration, and at 4 K the $H \perp$ TB configuration exhibited a bulklike response.

IV. CONCLUSIONS

Isothermal $M(H)$ curves exhibited two minima below 38 K. Above 12 K, the field position of the minima for the $H \parallel$ TB and $H \perp$ TB curves were quite similar. Below 12 K, the position of the second minimum occurred at a higher field value with $H \parallel$ TB. Below 6 K, only one minimum appeared for both field directions. At low temperatures, maxima in J_c occurred at the positions of the minimums in the $M(H)$ curves. Vortex lines were expelled more easily for $H \parallel$ TB than for $H \perp$ TB. At $T < 12$ K with $H \parallel$ TB, the relaxation rate for flux lines leaving the crystal was different from that for flux entering the crystal.

We also observed flux jumps in the magnetization curves at low temperatures, with their sizes depending whether H was applied parallel or perpendicular to the TB's. The studies indicated that TB's may act as oriented defects producing anisotropic flux jumping as vortex lines moved inside the sample.

ACKNOWLEDGMENTS

We want to acknowledge J. L. Tholence and E. H. Brandt for helpful discussions and W. Kwok for helpfull discussions and for suggesting the small-angle dependence experiment. The work at Argonne National Laboratory was supported by the U.S. Department of Energy, under Contract W-31-109-Eng-38. Work supported by CNPq and FAPESP, Brazilian agencies.

[1] M. Sarikaya and E. A. Stern, Phys. Rev. B **37**, 9373 (1988).
[2] G. P. E. M. van Bakel, P. A. Hof, J. P. M. van Engelen, P. M. Bronsveld, and J. Th. M. De Hosson, Phys. Rev. B **41**, 9502 (1990).
[3] J. Z. Liu, Y. X. Jia, R. N. Shelton, and M. J. Fluss, Phys. Rev. Lett. **66**, 1354 (1991).
[4] L. J. Swartzendruber, A. Roitburd, D. L. Kaiser, F. W. Gayle, and L. H. Bennett, Phys. Rev. Lett. **64**, 483 (1990).
[5] W. K. Kwok, U. Welp, G. W. Crabtree, K. G. Vandervoort, R. Hulscher, and J. Z. Liu, Phys. Rev. Lett. **64**, 966 (1990).
[6] C. A. Duran, P. L. Gammel, R. Wolfe, V. J. Fratello, D. J. Bishop, J. P. Rice, and D. M. Ginsberg, Nature (London) **357**, 474 (1992).
[7] E. M. Gyorgy, R. B. van Dover, L. F. Schneemeyer, A. E. White, H. M. O'Bryan, R. J. Felder, J. V. Waszczak, and W. W. Rhodes, Appl. Phys. Lett. **56**, 2465 (1990).
[8] M. Oussena, P. A. J. de Groot, S. J. Porter, R. Gagnon, and L. Taillefer, Phys. Rev. B **51**, 1389 (1995); M. Oussena, P. A. J. de Groot, K. Deligiannis, A. V. Volkozub, R. Gagnon, and L. Taillefer, Phys. Rev. Lett. **76**, 2559 (1996).
[9] V. K. Vlasko-Vlasov, L. A. Dorosinskii, A. A. Polyanskii, V. I. Nikitenko, U. Welp, B. W. Veal, and G. W. Crabtree, Phys. Rev. Lett. **72**, 3246 (1994).
[10] Rinke J. Wijngaarden, R. Griessen, J. Fendrich, and W. K. Kwok, Phys. Rev. B **55**, 3268 (1997).
[11] C. A. Duran, P. L. Gammel, D. J. Bishop, J. P. Rice, and D. M. Ginsberg, Phys. Rev. Lett. **74**, 3712 (1995).
[12] H. Pastoriza, S. Candia, and G. Nieva, Phys. Rev. Lett. **83**, 1026 (1999).
[13] J. A. Herbsommer, G. Nieva, and J. Luzuriaga, Phys. Rev. B **62**, 3534 (2000).
[14] G. A. Jorge and E. Rodriguez, Phys. Rev. B **61**, 103 (2000).
[15] A. V. Bondareko *et al.*, Low Temp. Phys. **27**, 339 (2001); *ibid.*, **27**, 201 (2001).
[16] P. Esquinazi, A. Setzer, D. Fuchs, Y. Kopelevich, E. Zeldov, and C. Assmann, Phys. Rev. B **60**, 12 454 (1999).
[17] R. G. Mints and E. H. Brandt, Phys. Rev. B **54**, 12 421 (1996).
[18] K.-H. Muller and C. Andrikidis, Phys. Rev. B **49**, 1294 (1994).
[19] M. Guillot, M. Potel, P. Gougeon, H. Noel, J. C. Levet, G. Chouteau, and J. L. Tholence, Phys. Lett. A **127**, 363 (1988).
[20] S. Salem-Sugui, Jr., A. D. Alvarenga, M. Friesen, B. Veal, and P. Paulikas, Phys. Rev. B **63**, 216502 (2001).
[21] C. P. Bean, Phys. Rev. Lett. **8**, 250 (1962).
[22] Michael Tinkham, *Introduction to Superconductivity*, 2nd ed. (McGraw-Hill, New York, 1996).
[23] M. C. de Andrade, N. R. Dilley, F. Ruess, and M. B. Maple, Phys. Rev. B **57**, R708 (1998).
[24] Y. Abulafia, A. Shaulov, Y. Wolfus, R. Prozorov, L. Burlachkov, Y. Yeshurun, D. Majer, E. Zeldov, and V. M. Vinokur, Phys. Rev. Lett. **75**, 2404 (1995).
[25] M. P. Maley, J. O. Willis, H. Lessure, and M. E. McHenry, Phys. Rev. B **42**, 2639 (1990).
[26] D. Shi and S. Salem-Sugui, Jr., Phys. Rev. B **44**, 7647 (1991).
[27] M. R. Beasley, R. Labash, and W. W. Weeb, Phys. Rev. **181**, 682 (1969).
[28] L. Burlachkov, Phys. Rev. B **47**, 8056 (1993); A. D. Alvarenga and S. Salem-Sugui, Jr., Physica C **235**, 2811 (1994).
[29] NIST WebHTS Data base [A. Junod *et al.*, Physica C **162–164**, 482 (1989); G. Triscone *et al.*, *ibid.* **168**, 40 (1990); J. Y. Genoud *et al.*, *ibid.* **177**, 315 (1991)].